ECCOMAS Congress 2016
VII European Congress on Computational Methods in Applied Sciences and Engineering
M. Papadrakakis, V. Papadopoulos, G. Stefanou, V. Plevris (eds.)
Crete Island, Greece, 5–10 June 2016

A PARAMETRICALLY TIME-DEPENDENT METHODOLOGY FOR RECIPROCATING CONTACT MECHANICS BETWEEN VISCOELASTIC SOLIDS

Carmine Putignano[1,2], Giuseppe Carbone[1,2], Daniele Dini[2].

[1]Department of Mechanics, Mathematics and Management,Politecnico di Bari, Bari, Italy.
e-mail address: carmine.putignano@poliba.it

[2] Department of Mechanical Engineering, Imperial College London, London, United Kingdom.

Keywords: Reciprocating motion, viscoelasticity, friction.

Abstract. *We implement an original Boundary Element methodology to study the reciprocating contact mechanics between linear viscoelastic materials. Results are shown for the case of a rigid sphere sinusoidally driven in sliding contact with a viscoelastic half-space. We observe the presence of multi-peaked pressure and displacement distributions; the hysteric friction curve is finally shown for different values of the frequency.*

1 Introduction

In modern engineering research, wide research efforts are dedicated to analyze and determine the mechanics and physics of soft linearly viscoelastic materials. The complexity of the topic is related to the strongly time-dependent and usually non-linear constitutive stress-strain relations that mark this class of materials. In particular, further complexity is added when soft bodies are brought into contact and the problem is exacerbated by the geometry of the intimately mating surfaces. As a matter of fact, a variety of publications has been dedicated to shed light on the contact mechanics of rough viscoelastic solids. Given the importance of the applications related to these issues[1, 2, 3], investigations performed across the scales, from macroscopic to atomistic levels, include analytical [4, 5] numerical [6, 7, 8, 9] and experimental [10, 11, 12, 13] studies.

In this paper, we focus on an issue that has been systematically ignored but has a particular importance: the reciprocating contact of viscoelastic materials, where the relative motion between the contacting bodies is periodically inverted. There is a countless number of engineering applications, ranging from the macro- to the nano- scales, where a periodic inversion of the motion direction is present. Earthquake viscoelastic dampers are a classic example [15, 15]: the design of these devices mostly relies on practical and empirical guidelines, and no tool for quantitative predictions is available. This lack of a robust theoretical framework affect different components, like all the sealing systems in mechanical applications with an alternate motion [14]. Indeed, enhancing performances and efficiency is infeasible without an accurate knowledge of the interfacial stresses and, consequently, of the dissipated power. Finally, reciprocating contacts have prominence also at different scales and in different contexts, like biology and biotechnology ([17],[18]). Skin, ocular system, joints, spine and vertebrae are some of the examples where viscoelastic soft contact occurs in the human body.

In this work, we present a Boundary Element Methodology that, for the first time, allow studying reciprocating contact mechanics between linearly viscoelastic solids and provide predictions of the response of the contacting surfaces in terms of stresses, strain and friction. The paper is outlined as follows. Section II describes the mathematical formulation which the numerical methodology relies on. Section III focuses on the reciprocating sliding contact of a sphere over a viscoelastic layer. Final remarks are included to comment on the relevance of the theory and of the results.

2 Formulation

We implement a Boundary Element Methodology to determine the contact solution and, specifically, stresses, strains and dissipation. It is well known that the general contact problem between a rigid indenter and a linearly viscoelastic slab may be formulated as:

$$u\left(\mathbf{x},t\right)=\int_{-\infty}^{t}d\tau\int d^{2}x\mathcal{J}\left(t-\tau\right)\mathcal{G}\left(\mathbf{x}-\mathbf{x}'\right)\dot{\sigma}\left(\mathbf{x}',\tau\right), \tag{1}$$

where $\mathbf{x}$ is the in-plane position vector, t is the time, $u\left(\mathbf{x},t\right)$ is the normal surface displacement of the viscoelastic slab, $\sigma\left(\mathbf{x},t\right)$ is the normal interfacial stress, $\mathcal{G}\left(\mathbf{x}\right)$ and $\mathcal{J}\left(t\right)$ are respectively the elastic Green's function and the creep material function. The relevance of such an approach is related to its generality: no assumption is made *a priori* on the shape of the contact domain and on the specific form of the linear viscoelastic response. As a consequence, the method can be employed for any kind of contact punch (conditions, like periodic boundaries and finite values of contacting layers thickness, can be easily managed [22, 8]) and for any kind of linear viscoelastic material, spanning from skin tissues to rubber-based composites.

However, tackling directly Eq. (1) is extremely challenging: because of the necessity of performing discretization both in time and space, the computational cost is huge, thus resulting infeasible with the computational technologies currently available. Consequently, when focusing our attention on the reciprocating contacts, we want to reduce the computational complexity of Eq. (1) without loosing its generality in terms of contact geometry and material properties. To this end, we assume that the interfacial normal stress distribution obeys the law $\sigma(\mathbf{x},t)=\sigma[\mathbf{x}-\xi_0\sin(\omega t)]$, i.e. that the shape of normal stress distribution is fixed but moves on the viscoelastic half-space with a sinusoidal law of amplitude $|\xi_0|$ and angular frequency ω. This enables us to rewrite Equation (1) as :

$$u(\mathbf{x},t)=\int d^2x' G(\mathbf{x}-\mathbf{x}',t)\,\sigma(\mathbf{x}'). \tag{2}$$

where, as shown in detail in Ref. [23], $G(\mathbf{x},t)$ is equal to:

$$G(\mathbf{x},t)=\sum_{k=-\infty}^{+\infty}\frac{A_k(\mathbf{x})}{E(k\omega)}e^{ik\omega t}. \tag{3}$$

where $A_k(\mathbf{x})$ can be written as

$$A_k(\mathbf{x})=(2\pi)^{-1}\int_{-1}^{1}ds\mathcal{G}(\mathbf{x}-s\xi_0)\,B_k(s) \tag{4}$$

with $B_k(s)$ being equal to $B_k(s)=(-i)^k T_k(s)\,B_0(s)$. $T_k(s)$ is the Chebyshev polynomial of the first kind and $B_0(s)=2\left(1-s^2\right)^{-1/2}$, for $|s|\leq 1$ and 0 otherwise.

As mentioned above, the function $G(\mathbf{x},t)$ relies on a precise assumption : we assume that the shape of the stress field at the interface, whose general form is $\sigma(\mathbf{x},t)=\sigma[\mathbf{x}-\xi_0\sin(\omega t),t]$, does not change during the reciprocating motion, *i.e.* $\sigma(\mathbf{x},t)=\sigma[\mathbf{x}-\xi_0\sin(\omega t)]$. Such a condition holds true whenever $a_0/|\xi_0|\ll 1$, where a_0 the characteristic dimension of the contact region, and is equivalent to require that $|\partial\sigma/\partial t|/(|\xi_0\cdot\nabla\sigma|\,\omega)\ll 1$ (the reader is referred to Ref. [23] for more details).

The solution of Eq. (2) can be pursued by employing the iterative technique developed in Ref. [21] for elastic contacts, thus providing contact areas, stresses, strains and, ultimately, the dissipated energy.

3 Results and discussion

In order to demonstrate the main features of the reciprocating contact, we study the contact of a rigid sphere of radius R undergoing reciprocating sliding against a viscoelastic material characterized by one relaxation time (being the ratio between the high frequency modulus and the low frequency $E_\infty/E_0=11$ and the Poisson ratio $\nu=0.5$). We assume that the center $\mathbf{x}(t)$ of the sphere moves on the viscoelastic half-space following the law $\mathbf{x}(t)=[\xi_0\sin(\omega t),0]$. The dimensionless angular frequency of the reciprocating motion is $\omega\tau=5$, being τ the relaxation time of the viscoelastic material.

For different values of $\omega t\in[-\pi/2,\pi/2]$, Figure 2 shows the evolution of the dimensionless displacements, $u(x)/R$, at the centre of the contact as a function of x/ξ_0 and for a specific dimensionless applied normal load $F_n/R^2E_0^*=0.014$, and $\xi_0/R=1$. An arrow refers, in each case, to the current position of the sphere. At $\omega t=-\pi/2$ the sphere has just reached the left dead-point and starts moving from left to right. Upon reversal of the sliding direction,

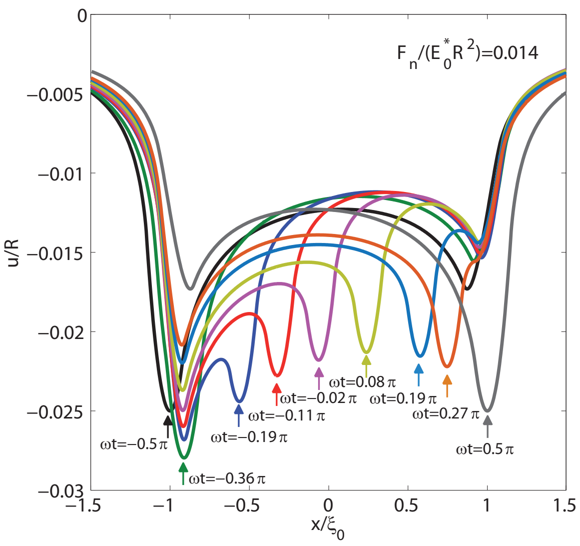

Figure 1: The dimensionless normal displacements $u(x, y = 0)/R$ as a function of the dimensionless abscissa x/ξ_0 for a constant dimensionless normal force $F_n/R^2E_0^* = 0.014$, for an amplitude $\xi_0/R = 1$ and for several values of the dimensionless time $\omega t \in [-\pi/2, \pi/2]$.

a marked increase of the dimensionless penetration at the center of the sphere is observed: although the speed is increasing, it is still too low to provoke a significant stiffening of the material, and the sphere is moving over a region of the viscoelastic half-space that has not yet had the time to relax after the previous contact of the rigid body. As the sliding speed increases, a non negligible stiffening of the material and a marked decrease of the penetration are observed (see displacement in correspondence to the arrow). Furthermore, additional deformation peaks appear: this is the result of the interplay between the deformations, induced by the indenter as it moves to the right, and the original not yet fully relaxed footprints left by the sphere at preceding times. For $0 < \omega t < \pi/2$, the sliding speed begins to decrease and the material softens again, thus leading to an increase of penetration. It is now possible to justify the occurrence of three different deformations peaks within the track when the sphere is moving between the two dead-ends: one corresponds to the current position of the sphere and the other two are located close to the left and right dead-points respectively, and are the result of the material inability to fully recover the viscoelastic deformations during a period of time comparable to the period $T = 2\pi/\omega = 6.28$ s of the reciprocating motion (recall that the relaxation time is $\tau = 5$ s).

The interplay of the sphere footprints, which occur at the dead-points of the reciprocating motion, has a significant effect on the interfacial normal stress distribution. This is clear in Figure 2, where contour plots of the pressure distribution are shown. Let us first notice that at $\omega t = -\pi/2$, *i.e.* when the sliding speed is equal to zero, the contact area as well as the interfacial normal stress distribution are characterized by an asymmetric shape. This is due to the viscoelastic time-delay which prevents the material to relax immediately when the sliding speed vanishes. As the sphere starts moving to the right, such a peak cannot disappear suddenly but has to show a gradual decrease. At the same time, since the punch is travelling towards the right, as already observed in steady-state viscoelastic contacts moving at constant velocity [7], a peak in the pressure distribution has to be originated also at the leading edge . Finally, at the center of the distribution, where we have the maximum of the displacement field in the contact area, the pressure must still resemble the classical elastic Hertzian solution. All this process strongly affects the evolution of the pressure distribution at the interface with the presence of

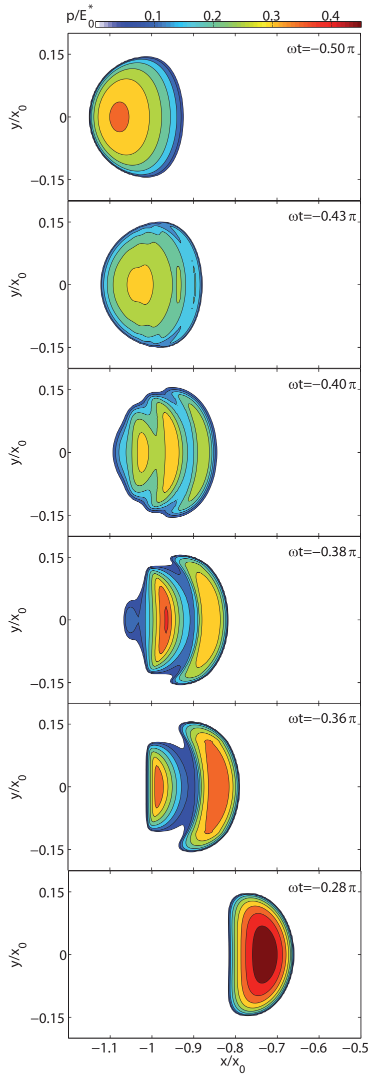

Figure 2: The shape of the contact area and the contour plots of the normalised contact pressure distributions, p/E_0^*, for several values of ωt .

multiple pressure peaks shown by the snapshots taken at $\omega t = -0.40\pi, -0.38\pi, -0.36\pi$.

Finally, in Figure 3, the reduced tangential force, F_t/F_n, easily calculated once pressures and displacements are known [7], is plotted as a function of the dimensionless abscissa x/ξ_0, which identifies the position of the sphere along the path, for different values of the parameter $\Xi = \omega\tau$. In detail, fixed the parameter $\Pi = \tau/t_0$ with t_0 being equal to $t_0 = a_0/\omega\tau$ -a_0 is the Hertzian radius-, for $\Xi = 0.1$ the material has the possibility to relax before a single reciprocating cycle is completed; consequently, the solution resembles the steady-state viscoelastic sliding contact and the tangential force F_t/F_n always opposes the sphere speed at each point along the path. However, as Ξ is increased the relaxation of the material involves time scales comparable to the time period of the reciprocating motion; in this case, there exist regions on the sphere track, specifically those close to the dead-points, where F_t/F_n has the same direction as the sliding speed. This is perfectly consistent with the results presented in Figure 2.

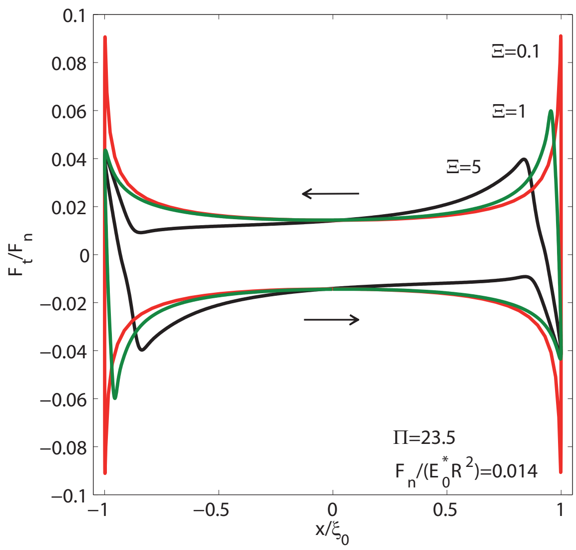

Figure 3: The ratio between the tangential and the normal force F_t/F_n as a function of the dimensionless abscissa x/ξ_0 for different values of Ξ . Arrows refer to the hysteresis cycle direction.

4 Conclusion

In this work, we present a Boundary Element Methodology capable of providing the full solution of the reciprocating contact problem between a rigid punch and a linear viscoelastic solid. The periodic features, intrinsically marking the problem, enables the parametric calculation of the contact solution for each time step without any necessity of employing the solution in the previous time interval. By implementing such a parametrically time-dependent approach, we obtain the full numerical convergence in each moment of the cycle and, interestingly, also when the punch inverts its motion.

For the simple case of a sphere in contact with a viscoelastic layer, we show that the behavior of the system is characterized by three peaks in the displacement distribution and, consequently, by multi-peaked pressure distributions. Finally, when calculating the dissipated energy, we observe that, for large values of the parameter Ξ, the tangential force F_t may have the same direction of the sliding speed.

Acknowledgements

CP gratefully acknowledges the support of Marie Curie Intra-European Fellowship SOFT-MECH (Grant No. 622632).

REFERENCES

[1] Arzt E. , Gorb S., and Spolenak R., From micro to nano contacts in biological attachment devices. Proceedings of the National Academy of Sciences, 16, 100 , 19 , 10603–10606, (2003).

[2] Bao G. , Suresh S., Cell and molecular mechanics of biological materials, Nature Materials 2, 715 - 725, (2003).

[3] Johannessen W., Vresilovic E. J., Wright A. C., Elliott D. M., Intervertebral Disc Mechanics Are Restored Following Cyclic Loading and Unloaded Recovery. Annals of Biomedical Engineering, 32, 1, 70-76, (2004).

[4] Hunter S.C. , The rolling contact of a rigid cylinder with a viscoelastic half space . Trans. ASME, Ser. E, J. Appl. Mech. 28, 611–617 (1961).

[5] Persson B.N.J., Theory of rubber friction and contact mechanics, Journal of Chemical Physics, 115, 3840 -3861, (2001).

[6] Dapp, W.B., Lücke, A., Persson, B.N.J., Müser, M.H., Self-affine elastic contacts: Percolation and leakage, Physical Review Letters, 108 (24), 244301, (2012).

[7] Carbone G. , Putignano C., A novel methodology to predict sliding/rolling friction in viscoelastic materials: theory and experiments., Journal of Mechanics and Physics of Solids, Journal of the Mechanics and Physics of Solids, 61 (8), 1822-1834, (2013).

[8] Putignano C. , Carbone G. , Dini D., Mechanics of Rough Contacts in Elastic and Viscoelastic Thin Layers, International Journal of Solids and Structures, 69–70, 507–517, (2015).

[9] Carbone G. , Putignano C.. Rough viscoelastic sliding contact: theory and experiments. Physical Review E, 89, 032408, (2014).

[10] Grosch K. A. , The Relation between the Friction and Visco-Elastic Properties of Rubber, Proceedings of the Royal Society of London. Series A, Mathematical and Physical, 274-1356, 21-39, (1963).

[11] Putignano C., Reddyhoff T., Carbone G., Dini D., Experimental investigation of viscoelastic rolling contacts: a comparison with theory. Tribology Letters , 51, 105–113, (2013).

[12] Putignano C., Le Rouzic J., Reddyhoff T. , Carbone G., Dini D. , A Theoretical and Experimental Study of Viscoelastic Rolling Contacts Incorporating Thermal Effects, Proceedings of the Institution of Mechanical Engineers, Part J: Journal of Engineering Tribology, vol. 228, no. 10, 1112-1121, (2014).

[13] Putignano C., Reddyhoff T. , Dini. D. The influence of temperature on viscoelastic friction properties. Tribology International, doi:10.1016/j.triboint.2016.03.018, (2016).

[14] Thatte A., Salant R. F., Effects of multi-scale viscoelasticity of polymers on high-pressure, high-frequency sealing dynamics, Tribology International, 52, 75–86, (2012).

[15] Shukla A. and Datta T. , Optimal Use of Viscoelastic Dampers in Building Frames for Seismic Force. Journal of Structural Engineering, 125 (4), 401–409, (1999).

[16] Takewaki I. Building Control with Passive Dampers: Optimal Performance-based Design for Earthquakes, John Wiley & Sons, (2011).

[17] Angelini T. E. , Dunn A. C., Uruena J. M., Dickrell D. J., Burris D. L. and Sawyer W. G. , Cell Friction, Faraday Discussion , 156, 31–39, (2012).

[18] Dunn A. C., Cobb J. A., Kantzios A. N., Lee S. J. , Sarntinoranont M. , Tran-Son-Tay R. , Sawyer W. G. , Friction Coefficient Measurement of Hydrogel Materials on Living Epithelial Cells, Tribology Letters, 30, 1,13-19, (2008).

[19] Christensen R. M., Theory of viscoelasticity, Academic Press, New York, (1982).

[20] Johnson, K.L.J., Contact Mechanics, Cambridge University Press, (1985).

[21] Putignano C., Afferrante L. , Carbone G., Demelio G. , The influence of the statistical properties of self-affine surfaces in elastic contact: a numerical investigation, Journal of Mechanics and Physics of Solids, 60, 5, 973–982, (2012).

[22] Carbone G., Mangialardi L., Analysis of adhesive contact of confined layers by using a Green's function approach, The Journal of the Mechanics and Physics of Solids, **56** (2), 684-706 (2008).

[23] Putignano C., Carbone G.,Dini D. : Theory of Reciprocating Contact for Viscoelastic Solids Accepted on Physical Review E (2016).